INTERNATIONAL JOURNAL OF CLIMATOLOGY
Int. J. Climatol. **25**: 913–930 (2005)
Published online in Wiley InterScience (www.interscience.wiley.com). DOI: 10.1002/joc.1172

REGIME SHIFT IN THE GLOBAL SEA-SURFACE TEMPERATURES: ITS RELATION TO EL NIÑO–SOUTHERN OSCILLATION EVENTS AND DOMINANT VARIATION MODES

SAYAKA YASUNAKA* and KIMIO HANAWA
Department of Geophysics, Tohoku University, Sendai, Japan

Received 2 May 2004
Revised 7 September 2004
Accepted 28 September 2004

ABSTRACT

Significant changes of mean state appearing widely in the global sea-surface temperature (SST) anomaly field have happened five times from the 1910s to the 1990s: 1925, 1942, 1957, 1970 and 1976. Since the regions of change spread over both hemispheres and/or multiple oceanic basins, they can be considered as 'global regime shifts'. The years of regime shifts are consistent with those of the Northern Hemisphere regime shifts reported by previous studies.

It is also shown that the regime shifts have happened concurrently with El Niño–southern oscillation (ENSO) events, which seems to suggest that the ENSO event acts as a trigger of the regime shift. At the regime shift, the tropical Pacific SSTs change from La Niña (El Niño) to El Niño (La Niña) conditions within 1 year. Further, the ENSO events occur just after the regime shifts begin in the July to September (JAS) season and reach the mature phase in the January to March (JFM) season as a typical evolution of the ENSO events. After that, they continue to at least the next year.

The five regime shifts detected have similar features in their seasonal evolution and persistence of signals. First, the shifts start in the JAS season: an SST change occurs in the eastern and central tropical Pacific, and a change in the mid-latitudes of the North and South Pacific appears with the opposite sign. Then the shifts in the JFM season. The spatial patterns are similar to those of the JAS season, but signals in the North Pacific become remarkable. These features resemble those corresponding to a series of evolutions of ENSO events, but the signals in the North Pacific and the North Atlantic are much stronger than those of the typical ENSO events. After the shifts have happened, the changes in spatial patterns of SST that occurred at the regime shift persist until the next shift. The persistence of signals is more prominent in the JFM season than in the JAS season.

From a review of the dominant variation modes in global SSTs using empirical orthogonal function (EOF) analyses, four modes are identified: the ENSO mode, the Southern Hemisphere trend mode, the North Pacific (NP) mode, and the Arctic oscillation (AO) mode. In the years when regime shifts occur, the ENSO mode, the NP mode, and the AO mode show significant concurrent phase reversals on the global scale as previously shown in the Northern Hemisphere. These findings provide a possible reason why SST changes in the regime shift are similar but not exactly the same pattern as that of ENSO. Furthermore, it can be considered that a simultaneous phase reversal of the NP mode would suppress the growth of anticyclonic (or cyclonic) circulation in the atmosphere over the western tropical Pacific. This suggests that an ENSO event, which begins with a regime shift, would not reverse its condition and last for the following several seasons.

KEY WORDS: regime shift; sea-surface temperature (SST); El Niño–southern oscillation (ENSO)

1. INTRODUCTION

Decadal-scale climate variations in the Northern Hemisphere (NH) ocean–atmosphere system have been documented by numerous studies (e.g. Kushnir, 1994; Mantua *et al*., 1997). The phase reversals of such decadal-scale variations are characterized as abrupt changes of sea-surface temperature (SST) and sea-level pressure (SLP) anomalies, called 'regime shifts' or 'climate jumps' (e.g. Nitta and Yamada, 1989; Minobe,

* Correspondence to: Sayaka Yasunaka, Department of Geophysics, Graduate School of Science, Tohoku University, Aoba-ku, Sendai 980-8578, Japan; e-mail: yasunaka@pol.geophys.tohoku.ac.jp

1997). Actually, Yasunaka and Hanawa (2002) detected six regime shifts during the period from the 1910s to the mid 1990s. Studies have also pointed out that the decadal-scale variations accompany the variations in SSTs and atmospheric circulation fields in the Southern Hemisphere (SH; e.g. Garreaud and Battisti, 1999; Tanimoto and Xie, 1999). Luo and Yamagata (2001) suggested that the SH plays a key role in the Pacific decadal variation.

Several characteristic patterns are known in the atmospheric circulation fields in the SH. The leading mode in the SH lower troposphere shows a strong zonal symmetry with a phase reversal between geopotential height anomalies in high- and mid-latitudes (e.g. Rogers and van Loon, 1982). This mode shows a decreasing trend of the lower tropospheric geopotential height over Antarctica (Mo, 2000; Thompson and Wallace, 2000). On the other hand, a wave train extending from the Pacific to the South American continent associated with an El Niño–southern oscillation (ENSO) event is identified, and called the Pacific–South American (PSA) pattern (e.g. Karoly, 1989), which is the counterpart of the well-known Pacific–North American (PNA) pattern in the NH. Although it has been shown that the variations in the atmospheric circulation pattern link to global SST anomalies (Mo, 2000), the relationship between the variation in the NH and that in the SH has not been clarified yet. In this study, we describe the spatio-temporal structures of the decadal-scale variations and the regime shifts on the global scale.

The ENSO-related SST mode changes its sign at regime shifts (Overland *et al*., 2000; Yasunaka and Hanawa, 2003). The ENSO and decadal-scale components of the subsurface temperature variations in the eastern equatorial Pacific also show a simultaneous phase reversal during the period from 1976 to 1977 (Luo and Yamagata, 2001). Recently, Masuda (2002), executing numerical experiments with a low-order model, has suggested that the ENSO events affect the decadal-scale variation in the North Pacific. Therefore, the purpose of this study is to investigate the relationship between the ENSO events and the regime shifts, using gridded observational SST data.

It is well known that dominant SST variations and atmospheric teleconnection patterns have different spatial patterns among the seasons (e.g. Barnston and Livezy, 1987; Tanimoto *et al*., 1997). Since the seasons are reversed between the NH and the SH, the dominant variations in the NH winter season, such as the PNA teleconnection pattern or the North Atlantic oscillation (NAO), do not always represent the global-scale variations appropriately. Furthermore, since the evolution of ENSO events is phase locked to the annual cycle (Rasmusson and Carpenter, 1982; Horii and Hanawa, 2004), features of the ENSO events cannot be captured in an annual mean state. In this study, analyses are performed for each season separately, and we describe the seasonal evolutions of the regime shifts. Since global variation modes in previous studies were detected by analyses using annual mean anomalies or all monthly anomalies irrespective of seasons (e.g. Kawamura, 1994; Kaplan *et al*., 2000; Smith and Reynolds, 2002), we also reanalyse the dominant variation modes in the global SSTs and investigate the relationship between those modes and the regime shifts.

The remainder of this paper is organized as follows. The data used are outlined in Section 2. In Section 3, we detect the years when discontinuities of SST anomalies occurred over a wide area of the global oceans (i.e. regime shifts), and investigate the temporal evolutions of the changes and the persistence of signals, comparing with those of the ENSO event. In Section 4, dominant SST variation modes over the globe are clarified by empirical orthogonal function (EOF) analyses, and their changes at the regime shifts detected in Section 3 are examined. Section 5 gives our conclusions.

2. DATA

The monthly mean SST data are computed from the Comprehensive Ocean–Atmosphere Data Set (COADS; Woodruff *et al*., 1987), National Centers for Environmental Prediction (NCEP) real-time marine observations by NOAA/Climate Diagnostics Center, and the Kobe Collection (Manabe, 1999; see Yasunaka and Hanawa (2002)). Although the SST data span the period from 1854 to 2002, we use only the data after the 1910s, when the data coverage spreads over basins, especially along the main shipping routes. In order to confirm that results do not depend on the data processing, the SST dataset (extended reconstructed SST; ERSST)

prepared by Smith and Reynolds (2002) and the global sea-ice and SST (GISST) dataset archived at the Hadley Centre (Rayner *et al*., 1996) are also used. In this study, we will mainly show the results using our dataset, but discuss only the features that appear in all three datasets.

Atmospheric data, such as SLP and sea-surface wind (SSW), are monthly means from the NCEP–National Center for Atmospheric Research (NCAR) reanalysis (Kalnay *et al*., 1996). The data cover the period from 1948 to 2001. Since observations are very limited in the early period over the high latitudes of the SH, observational station SLP data (Jones and Limbert, 1987) are also used to confirm the results.

In this study, seasonal means are calculated from the monthly data. Each season is defined as the three consecutive months, from January to March (JFM) and from July to September (JAS) for the SST data, and from December to February and from June to August for the atmospheric variables. These months correspond to the periods having peak winter and summer conditions in the respective fields. Since the seasons are opposite between the NH and the SH, we call these 3-month periods the JFM or JAS season, instead of winter or summer, not only for the SST but also for the atmospheric variables.

3. REGIME SHIFT AND ENSO EVENT

3.1. Detection of global regime shifts

In this study, we define a significant SST change in the global ocean as a regime shift. That is, the change is regarded as a regime shift when many grids simultaneously show significant change, and the changes spread into a wide area. In order to detect the years when regime shifts occurred, we apply the 'multiple change points test', which can objectively identify discontinuities in time series (Lanzante, 1996). Although the analysis period is from 1910 to 2002, this method cannot detect appropriately in the first and last 10 years, because the reliability of this detection method is low at the ends of a time series.

Figure 1(a) shows the percentage of grids having significant changes at the 90% significance level to the data-filled grids in the SST field in the JFM season. We obtain 12 years whose percentages exceed the sum of the mean and the standard deviation (shown by a dashed line); 1925–26, 1930–31, 1941–42, 1942–43, 1945–46, 1946–47, 1956–57, 1957–58, 1970–71, 1976–77, 1977–78, 1987–88. In order to reduce uncertainty by processing of the dataset, the same analyses are applied using ERSST and GISST, which are made by different interpolation and bias-correction methods. As a result, 14 years are detected from ERSST and 10 years from GISST. Then we consider regime shifts that happened at 5 years that are detected from all three datasets, i.e. 1925–26, 1942–43, 1957–58, 1970–71, and 1976–77. We omitted 1977–78 from regime shift years, since changes in 1977–78 are the same sign as those of 1976–77 but they are weaker than those in 1976–77 in most regions. Here, note that the number of years detected is less than that expected from the data length and the significance level (e.g. 10 years in a 100 year record at the 90% significance level). Actually, a Monte Carlo simulation based on a random sampling model using 1000 surrogate time series showed that about 2.5% of the JFM global SST grids show significant changes at the 99% confidence level in each year. This percentage is comparable to the average percentage of change grids in the actual SST data. Therefore, it cannot be said that five-time changes in a near 100 year record detected in the present study happened by chance.

In order to confirm the regime shifts detected above that appeared widely in the global ocean, the same time series as Figure 1 are prepared for several sub-regions. Considering the oceanic domain directly influenced by the tropics (Hadley cell in the atmosphere and propagation nature of oceanic heat contents from the tropics in the ocean (Hasegawa and Hanawa, 2003)), the region between 20 °N and 20 °S was regarded as the tropics, and the regions north of 20 °N and south of 20 °S were regarded as the extratropics of each hemisphere. That is, nine sub-regions are defined: the North (north of 20 °N), South (south of 20 °S), and tropical (20 °S–20 °N) Pacific, the north, south and tropical Indian Ocean, and the North, South and tropical Atlantic. Here, even if we choose 25° or 15° as the boundary, the results are not different from those of 20°. Although the time series for each of the sub-regions show diverse large percentage years, large percentages above the mean plus the standard deviation are found in the many sub-regions at the regime shifts previously detected (Table I). The North and South Pacific and tropical Indian Ocean show large percentages at almost all regime shifts.

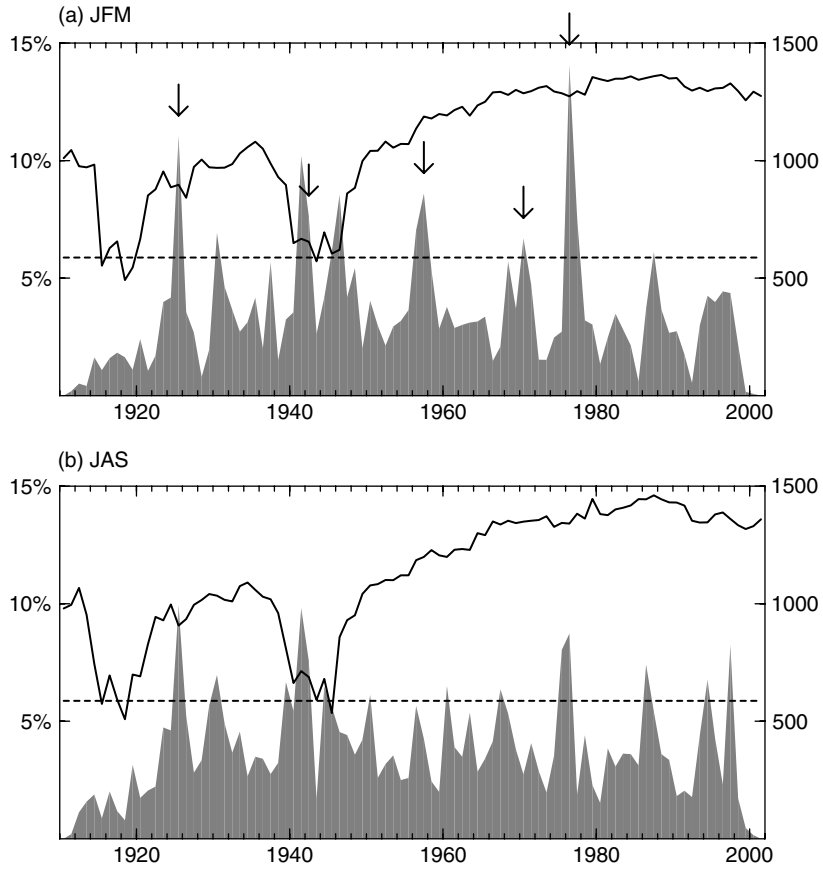

Figure 1. Time series of percentage of the grids showing significant discontinuities at 90% significance level to the data-filled grids in the SST field in the globe in (a) the JFM season and (b) the JAS season (shading). Dashed line denotes the mean plus the standard deviation of percentages from 1910–11 to 2001–02. Solid line is the number of data-filled grids. The years shown by arrows are those detected as the global regime shifts (see text)

Table I. Sub-regions in which percentages of the grids showing significant discontinuities at the 90% significance level to the data-filled grids are above their mean plus standard deviation at the regime shift years in the JFM season. Nine sub-regions are defined: the North (north of 20 °N), South (south of 20 °S), and tropical (20 °S–20 °N) Pacific (NP, SP, and TP), the North, South and tropical Indian Ocean (NI, SI, and TI), and the North, South and tropical Atlantic (NA, SA, and TA)

Shift year	Shift region
1925–26	NP, TP, TI, NA, TA
1942–43	NP, SP, NI, SI, TI
1957–58	NP, SP, TP, SI, TI, TA
1970–71	SP, NA, TA
1976–77	NP, SP, TP, TI, NA, SA

On the other hand, the north Indian Ocean and South Atlantic are included only at one shift. Although shift regions are different at each regime shift, not only more than half of the sub-regions show large percentages, but also shift regions spread over both hemispheres and/or multiple oceanic basins. Using the other SST datasets, large percentages also appear in the majority of sub-regions in those years, although the numbers of sub-regions showing large percentages at each shift are slightly different. This means that the changes at the regime shifts detected above appeared widely in the global ocean. Therefore, they can be considered as global regime shifts.

In the JAS season (Figure 1(b)), although 5 years are detected from three datasets (1925–26, 1930–31, 1941–42, 1975–76, 1976–77), less than four sub-regions among nine show large percentages in all of them. Furthermore, they do not seem to show a prominent relation with those in the JFM season. This means that significant changes in the JAS season did not appear in the global ocean and that the global regime shifts cannot be defined well in the JAS season.

We mentioned that the global regime shifts were detected only in the JFM season, but they did not appear as the global regime shifts in the JAS season. This fact is consistent with the feature that the decadal-scale variation is prominent in the JFM season (e.g. Tanimoto *et al*., 1997; Watanabe and Kimoto, 2000). Since winter SST anomalies are isolated under the stable seasonal thermocline in summer (e.g. Namias and Born, 1970; Alexander and Deser, 1995; Hanawa and Sugimoto, 2004), it is considered that variations are not necessarily the same between the two seasons.

The regime shifts detected here are consistent well with the NH regime shifts already reported by previous studies (Overland *et al*., 1999; Yasunaka and Hanawa, 2002). In particular, the 1976–77 shift has been noted and described by many studies (e.g. Nitta and Yamada, 1989; Trenberth, 1990). The 1920s and 1940s shifts are known as an interdecadal change of the Aleutian low (AL) intensity (e.g. Mantua *et al*., 1997; Minobe, 1997). The 1957–58 shift in the North Pacific and tropical Indian Ocean SSTs was pointed out by Zhang *et al*. (1997). In the early 1970s, the NAO index exhibited a sharp reversal from a downward trend (Hurrell, 1995). The 1988–89 regime shift was also pointed out by many previous studies, as well as the other shifts (Tachibana *et al*., 1996; Yasunaka and Hanawa, 2002). However, since changes in 1988–89 are confined in the NH in the JFM season and have almost no signal in the SH, it is not regarded as a regime shift in the global ocean (not shown here) in the present study. Yasunaka and Hanawa (2003) also described the difference between the 1988–89 shift and other shifts from the viewpoint of tropical variations.

Data coverage is poor during last half of the 1910s and the whole of the 1940s, especially in the South Pacific, the North and South Indian Ocean, and the South Atlantic. Although ERSST and GISST have no missing grids by interpolations, the certainty of these periods is low (Smith and Reynolds, 2003). Therefore, the shifts in 1942–43 in the South Pacific, and the North and South Indian Ocean are not so reliable as others.

3.2. Seasonal evolution of regime shifts and its relation to ENSO events

Figure 2 shows time series of the Niño-3.4 index (SST anomalies averaged for 5 °N–5 °S, 170–120 °W; Trenberth, 1997). The Niño-3.4 index is known as the index of the ENSO event, and El Niño and La Niña are defined by continuingly exceeding ±0.4 °C for 6 months or more (small arrows; Trenberth, 1997). It is found that all the regime shifts (vertical lines) happened concurrently with ENSO events.

Table II summarizes the temporal evolutions of the ENSO events. Although the majority of ENSO events begin in the JAS season 1 year before the mature phase (shown as JAS (−1) in the third column of Table II; 16 cases in 34 events) and retain their mature phase in the JFM season (JFM in the fourth column; 22 cases), a series of the evolution of ENSO events shows various combinations, which is known as an irregular aspect of the ENSO events (e.g. Neelin *et al*., 2000; Horii and Hanawa, 2004). However, among the ENSO events just after the regime shifts (shown by bold numbers in Table II), two of them (1943 and 1958) show '−−, JAS (−1), JFM, +' (see Table II), and the remaining three events also show almost the same evolutions (only one element is different). That is, at the regime shifts, the tropical Pacific SSTs change from La Niña (El Niño) to El Niño (La Niña) conditions within 1 year, then the ENSO events just after the regime shifts begin in the JAS season, retain the mature phase in the JFM season, and continue to at least the next year. On the other hand, among all of 34 ENSO events, the ENSO events showing those seasonal evolutions are only nine

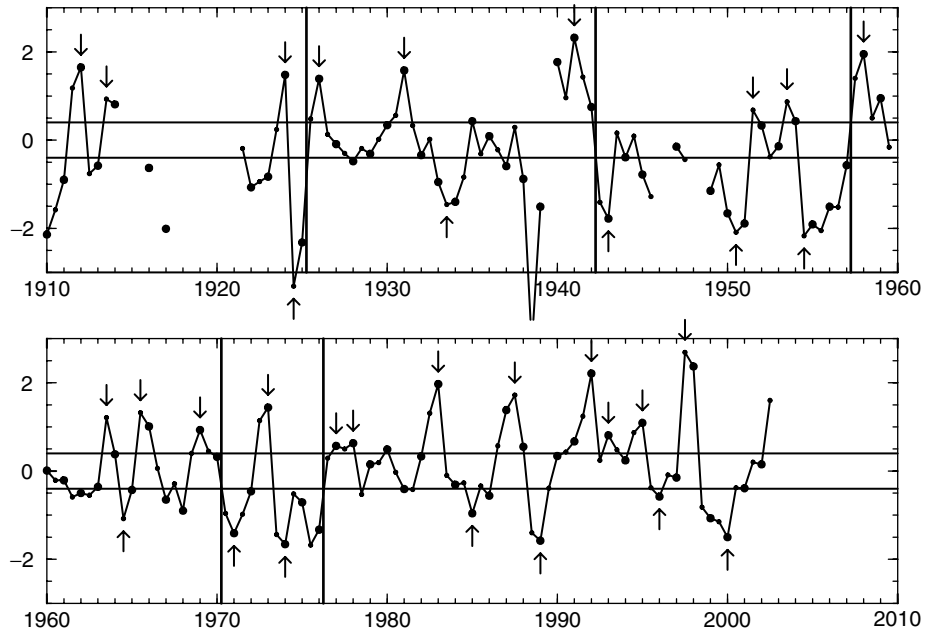

Figure 2. Time series of the Niño-3.4 index. Large (small) circles denote JFM (JAS) season. Horizontal lines are ±0.4 °C. The years shown by vertical lines are those detected as the regime shifts. Small arrows are the year when the ENSO events occurred (Trenberth, 1997)

(4 in 28 events, except for the events just after the regime shifts). This implies that the regime shifts closely relate to the temporal evolution of the ENSO events, and the regime shifts that happened in global SSTs in the JFM season have already begun in the JAS season of the previous year.

Now, a seasonal evolution of the spatial patterns of the regime shifts is explored. Figure 3 shows composites of SST and SSW anomalies before and after the five regime shifts (1925, −1942, 1957, −1970, 1976; the shifts of 1942 and 1970 are composed after the signs of anomalies are reversed). As a whole, signs of anomalies are reversed at the regime shifts in the global ocean. That is, SST and SSW fields change from the La Niña-like condition to the El Niño-like condition at the regime shifts, as well as the Niño-3.4 index. The shifts start in the JAS season. Changes occur in the eastern and central tropical Pacific, and changes in the mid-latitudes of the North and South Pacific appear with an opposite sign to those in tropical areas. Then the shifts in the JFM season follow. The spatial patterns are similar to those of the JAS season, but the amplitudes of the anomalies in the North Pacific are larger. In the Indian Ocean, negative SST anomalies 1 year before the regime shifts decay in the JAS season of the shift year and positive anomalies appear in the following JFM season. In the North Atlantic, negative SST anomalies in the western mid-latitudes and easterly wind in the high-latitudes corresponding to the weakening of the Icelandic low, which are opposite features 1 year before the regime shifts, become prominent in the JFM season of the shift year. The features of the seasonal evolutions are similar to those of each regime shift.

Figure 4 shows a seasonal evolution of the general ENSO events. In order to compare easily with the regime shifts, contour intervals are standardized by the ratio of the Niño-3.4 index in the JFM season. First, tropical Pacific SSTs become warm in the JAS season from the eastern part, and then the maximum SST anomalies expand westward into the central region, as already known (Rasmusson and Carpenter, 1982). Changes in the mid-latitudes of the North and South Pacific appear with an opposite sign to those in the tropical zone. These features are similar to those of the regime shifts. However, even if the signals are standardized by the magnitude of the Niño-3.4 index, the North Pacific and the North Atlantic mid-latitude responses of the ENSO event are weaker than those of the regime shifts, which are consistent with the features of the ENSO-like decadal variation (Zhang *et al*., 1997). On the other hand, there is no marked difference between the regime shifts and the ENSO event in the South Pacific. Whereas a typical La Niña condition appears 1 year before

Table II. Temporal evolutions of the ENSO events. The season when the magnitude of the Niño-3.4 index shows a maximum value is defined as the peak season, and the season when it exceeds 0.4 °C is defined as the onset season. The conditions 1 year before and after the peak season are also shown. '+ (−)' denote magnitude of the Niño-3.4 index exceeds 0.4 °C with the same (opposite) sign as that at the peak season, and '0' denotes magnitude of the Niño-3.4 index is less than 0.4 °C. '++ (−−)' denotes the previous event of the same (opposite) sign. '?' means no data

Year	Previous year	Onset	Peak	Next year
1912	−−	JAS (−1)	JFM	−
1913	−	JAS	JAS	?
1924	−	JFM	JFM	−
1925	−−	JAS	JAS	−
1926	−−	JAS (−1)	JFM	0
1931	0	JAS (−1)	JFM	0
1933	0	JFM	JAS	+
1938	+	JFM	JAS	+
1941	+	JFM (−1)	JFM	+
1943	−−	JAS (−1)	JFM	+
1950	+	JAS (−1)	JAS	−
1951	−−	JAS	JAS	0
1953	0	JAS	JAS	−
1954	−−	JAS	JAS	+
1958	−−	JAS (−1)	JFM	+
1963	−	JAS	JAS	−
1964	−−	JAS	JAS	−
1965	−−	JAS	JAS	0
1969	−	JAS (−1)	JFM	0
1971	0	JAS (−1)	JFM	+
1973	−−	JAS (−1)	JFM	−
1974	−−	JAS (−1)	JFM	+
1977	−−	JFM	JFM	+
1978	++	JAS (−1)	JFM	0
1983	0	JAS (−1)	JFM	0
1985	0	JFM	JFM	+
1987	−	JAS (−1)	JAS	−
1989	−−	JAS (−1)	JFM	0
1992	+	JAS (−2)	JFM	+
1993	++	JFM	JFM	0
1995	0	JAS (−1)	JFM	−
1996	−−	JFM	JFM	0
1997	0	JAS	JAS	−
2000	+	JAS (−2)	JFM	0

the regime shifts, the La Niña-like features are much weaker 1 year before an ENSO event. As a result, it can be said that there are differences between the seasonal evolutions of the regime shifts and those corresponding to a series of the evolution of ENSO events, although several features are similar to each other.

In order to eliminate an influence of the strength of each ENSO event, we also make composite maps in which anomalies are standardized by the magnitude of the Niño-3.4 index in the peak season before composition. The features described above can also be observed in the standardized composites. This means that the differences between the seasonal evolution of the regime shifts and those of the general ENSO events are independent of the strength of the ENSO events.

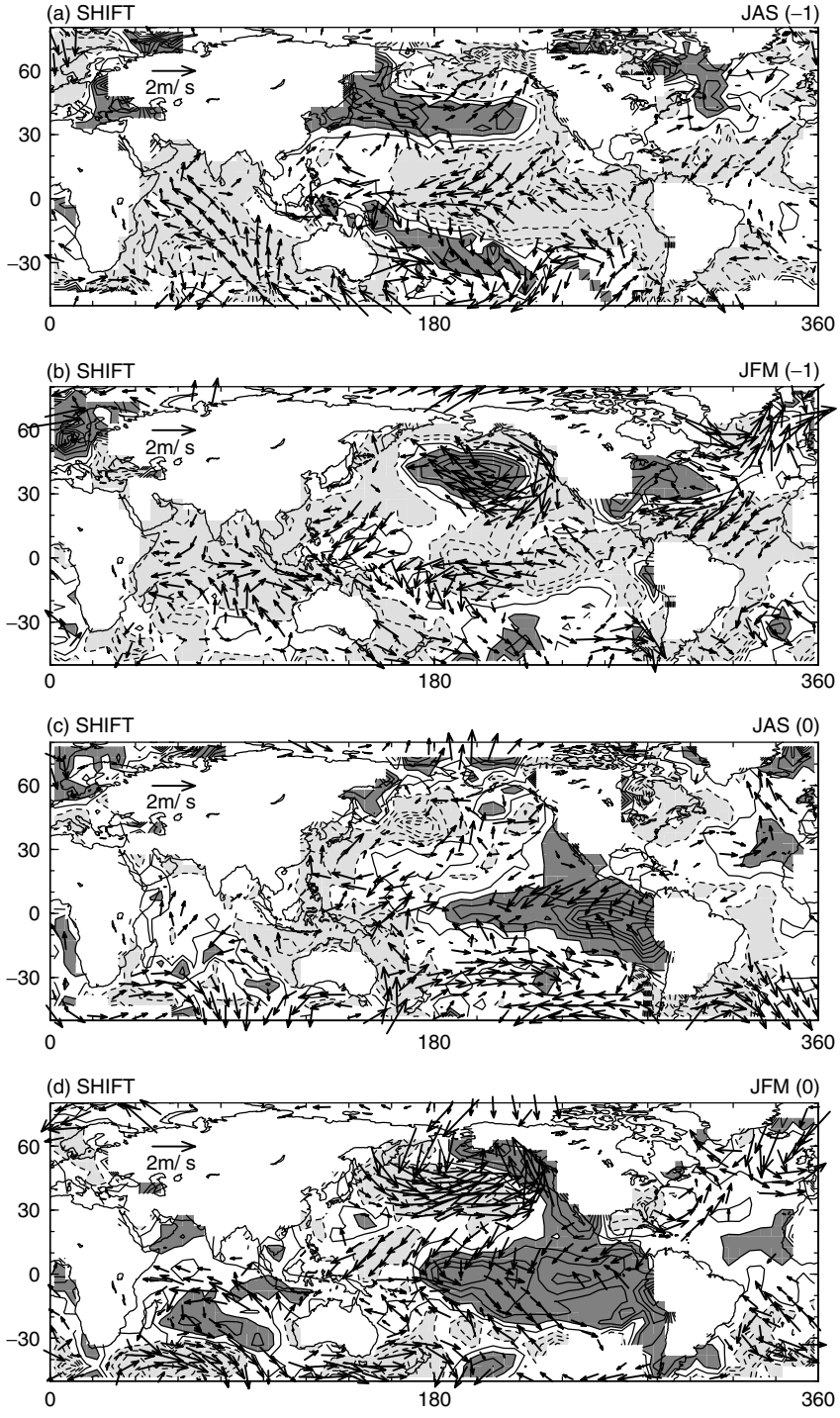

Figure 3. Composites of SST and SSW before and after the regime shifts (1925, −1942, 1957, −1970, 1976). The shifts of the opposite sign are composed after the signs of anomalies are reversed (the years with minus sign). For example, for the 1976 regime shift, (a) to (d) correspond to the 1975 JAS season, 1976 JFM season, 1976 JAS season, and 1977 JFM season respectively. Contour interval is 0.2 °C. Negative contours are dashed. Wind vectors are drawn only if the means of u (east–west component) or v (north–south component) exceed half of their standard deviations

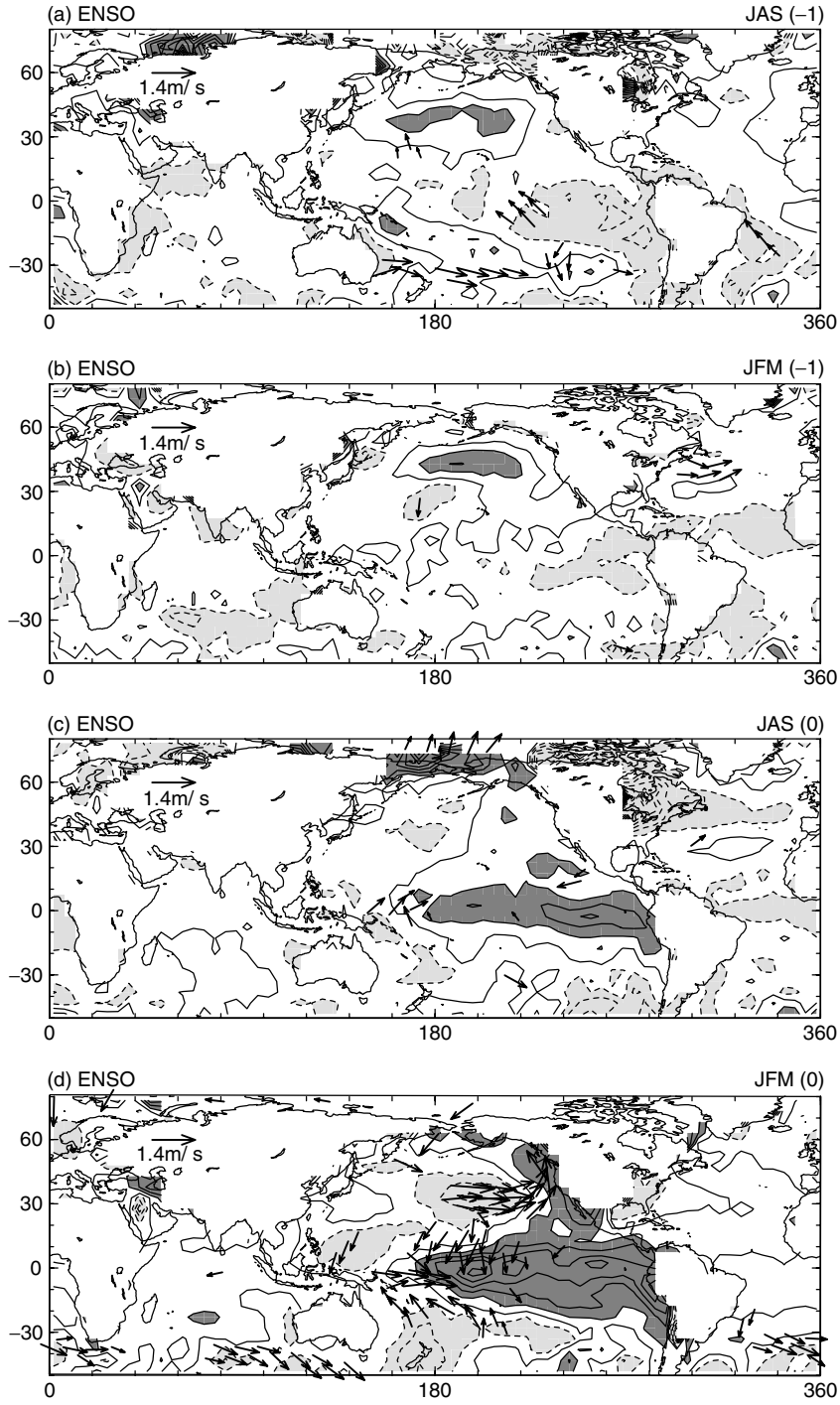

Figure 4. Composites of SST and SSW before and after the ENSO events (1912, 1913, 1924, −1924, 1926, 1931, −1933, −1938, 1941, −1943, −1950, 1951, 1953, −1954, 1958, 1963, −1964, 1965, 1969, −1971, 1973, −1974, 1977, 1978, 1983, −1985, 1987, −1989, 1992, 1993, 1995, −1996, 1997, −2000; Trenberth, 1997). The events of the opposite sign (i.e. La Niña) are composed after the signs of anomalies are reversed (the years with minus). For example, for the 1952 ENSO event, (a) to (d) correspond to the 1950 JAS season, 1951 JFM season, 1951 JAS season, and 1952 JFM season respectively. Contour interval is 0.14 °C. Negative contours are dashed. Wind vectors are drawn only if the means of u or v exceed half of their standard deviations

3.3. Persistence of shift signals

In order to clarify the persistency of signals changing at the regime shifts, composite difference maps are shown. Figure 5 shows composite difference maps of SST and SSW in the regime shift years (Figure 5(a) and (b)), and those between two successive periods from one regime shift to the next one (i.e. regimes) except for the regime shift years (Figure 5(c) and (d)). Signals happening at the regime shift persist until the next regime shift in the tropical Pacific, the central and eastern North Pacific, the mid-latitude of the South Pacific, the Indian Ocean, and all over the North Atlantic, even though the amplitudes are weakened. On the other hand, anomalies in the eastern equatorial Pacific, which show the largest SST change at the shift, decayed and became weaker or there were no signals. This is consistent with a previous study of the Niño-3.4 region (170–120 °W) that shows a stronger signal than the Niño-3 region (150–90 °W) in the decadal-scale variation (Hasegawa and Hanawa, 2003; Yasunaka and Hanawa, 2003). It is also found that the persistence of signals is more prominent in the JFM season than in the JAS season.

Figure 6 shows SLP difference maps between the two regimes. They show symmetric patterns about the equator. A west–east seesaw of SLPs corresponding to the southern oscillation is found in the tropics, with negative shifts in the eastern Pacific and positive ones in the other regions (the zero contours go across the equator near the Date Line in Figure 6). The PSA pattern is observed in the SH, corresponding to the PNA pattern in the NH. Whereas the polar region of the NH shows a positive change, the polar region of the SH has no signals. SLP differences in the summer hemispheres (not shown here) show similar patterns but smaller magnitudes than SLP differences in the winter hemispheres.

4. DOMINANT VARIATIONS IN THE GLOBAL SST FIELD AND THEIR RELATION TO REGIME SHIFTS

4.1. Dominant variation modes in the global SST field

In order to detect dominant modes of variations in the SST field, EOF analyses are applied by a covariance matrix method. Various analysis domains and/or periods are examined to extract meaningful spatial patterns and temporal variations. The analysis periods are 52 years from 1951 to 2002 for the NH, when the data are filled at almost all grids south of 60 °N, and 45 years from 1958 to 2002 for the SH, when the data are filled at almost all grids north of 40 °S. EOF time coefficients are extended until 1910 by a projection of SSTs onto the corresponding EOF spatial patterns. Taking into account the difference in the spatial patterns between the seasons, as mentioned in Section 1, we treat the JFM and JAS seasons separately.

As a result, four dominant modes, which correspond well with the well-known patterns in the ocean–atmosphere system, are detected. Figure 7 shows the time variations and spatial patterns.

The most dominant mode is referred to as the ENSO mode, as is already well known (e.g. Weare *et al*., 1976). This mode is obtained as the first EOF mode in both hemispheres in the JAS season and in the SH in the JFM season (the first mode in the NH in the JFM season is contaminated with other modes; see Yasunaka and Hanawa (2003)). Since the time coefficients of these EOF modes correlate well with the Niño-3.4 index, we use the Niño-3.4 index as the index representing the temporal variation of the ENSO mode. Further, we confirmed that the results were the same even if we chose any one of the EOF modes. The explained variances of the Niño-3.4 index are 19.1% in the JFM season and 19.8% in the JAS season. Figure 7(a) and (b) shows time series and SST regressions of the Niño-3.4 index. The SST spatial patterns show symmetric features about the equator, as shown by numerous studies (e.g. Trenberth and Caron, 2000). Several asymmetric features also exist: the Pacific mid-latitude signals having a negative sign extended further north and south in the winter hemisphere than those in the summer hemisphere. The signal in the eastern equatorial Pacific in the JAS season is stronger and more confined than that in the JFM season, and is consistent with the seasonal evolution of the ENSO event, as mentioned in the previous section. The correlation between the time coefficient of the JFM season and that of the JAS season of the previous year is very high ($R = 0.88$). This fact corresponds to the phase-locked features of the ENSO seasonal evolution. The regression maps of the atmospheric circulation fields are characterized by those related to the southern oscillation in the tropics

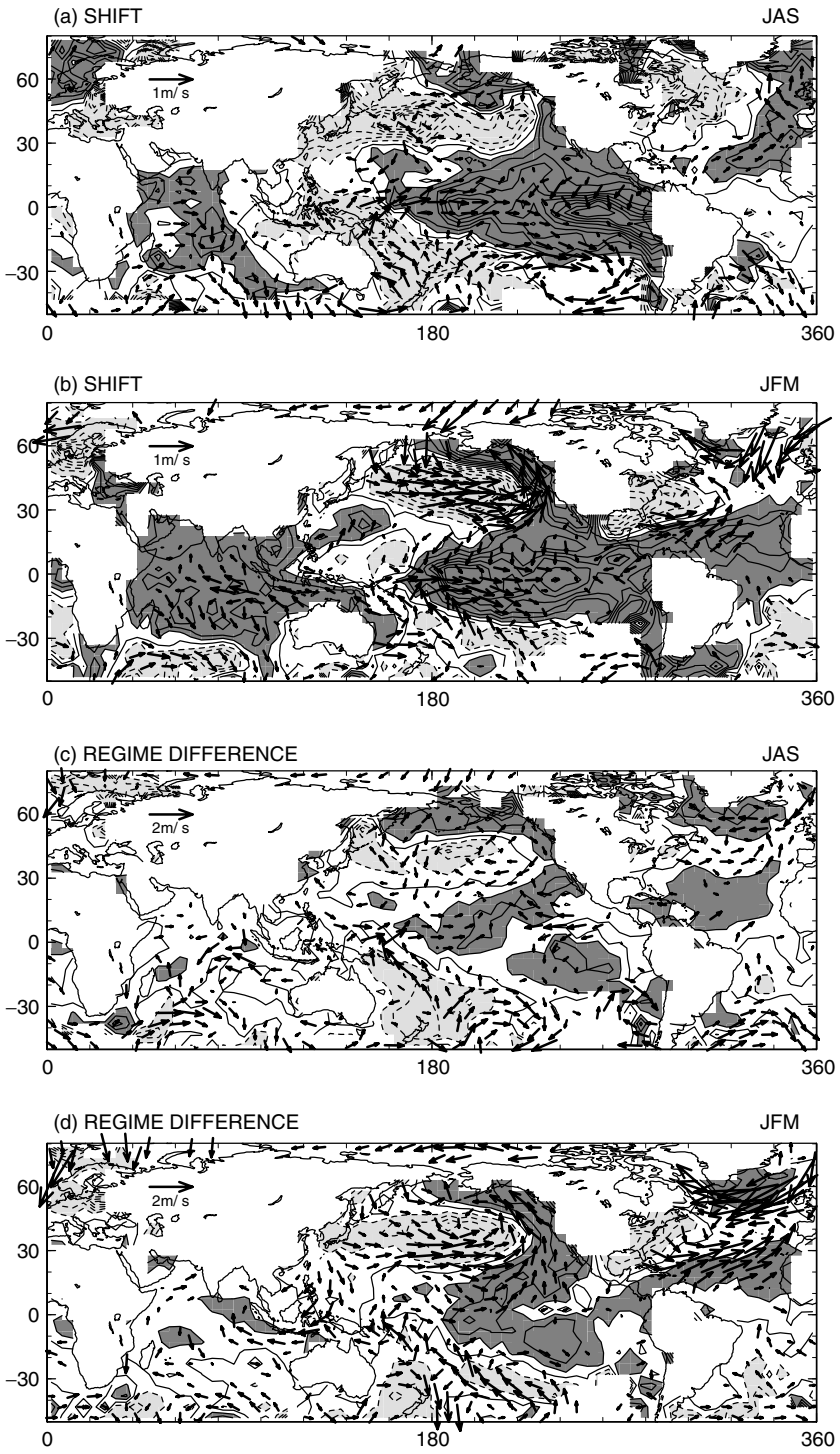

Figure 5. Composite difference maps of SST and SSW at the regime shift years (a and b), and those between the successive two regimes except for the regime shift years (c and d). For example, for the 1976 regime shifts, the shift difference (a and b) and regime difference (c and d) correspond with [1976] – [1975] and [1977 – 1986] – [1971 – 1974] in JAS, and [1977] – [1976] and [1978 – 1987] – [1972 – 1975] in JFM respectively. Contour interval is 0.2 °C. Negative contours are dashed. Wind vectors are drawn only if the means of u or v exceed their standard deviations

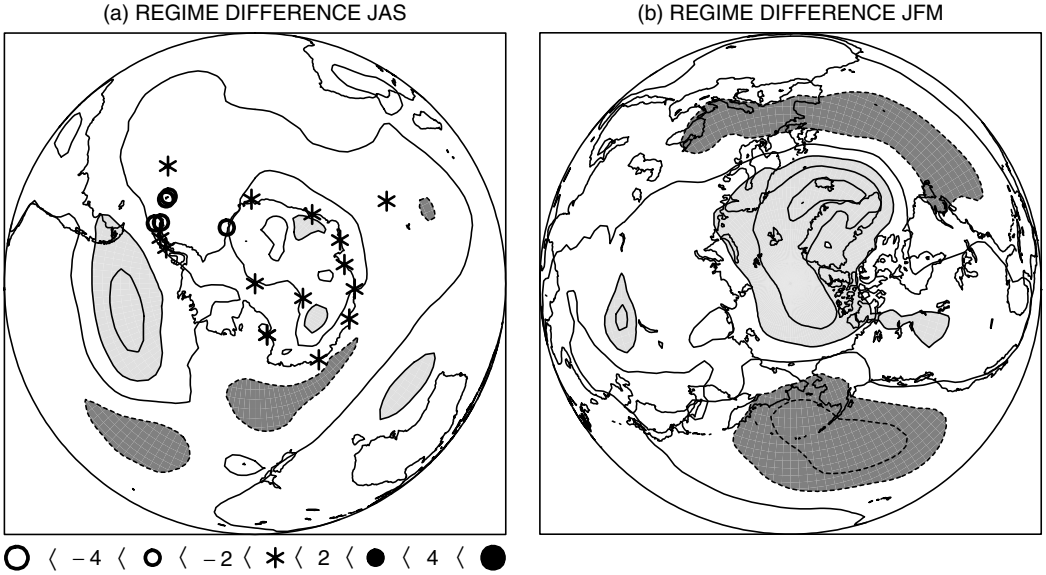

Figure 6. SLP composite map of difference between the successive two regimes including the regime shift years. Contour interval is 2 hPa. Negative contours are dashed

in both seasons, and the PNA (PSA) pattern in Pacific and North (South) American sectors in the JFM (JAM) season, as Karoly (1989) showed.

The second dominant mode is the SH trend mode (Figure 7(c) and (d)). This mode is obtained as the second EOF mode in the SH in both seasons. The explained variances in the global ocean are 10.2% in the JFM season and 14.0% in the JAS season. Time coefficients of these EOF modes show remarkable upward trends. SST regressions of both seasons show positive anomalies in the wider region. The atmospheric circulation fields show zonally elongated signals with opposing signs between mid latitudes (low and mid latitudes) and high latitudes in the JFM (JAS) season. This feature is known as the leading mode of the SH extratropical circulation (e.g. Rogers and van Loon, 1982; Karoly *et al*., 1996) called the 'annular mode' (Thompson and Wallace, 2000). Smith and Reynolds (2002) also found a warming trend in the SH mid-latitudes beginning around 1930. Thompson *et al*. (2000) pointed out that the trend of the SH annular mode was consistent with the recent decreasing trend of the SH total column ozone.

The third and fourth dominant modes are the North Pacific (NP) mode (Figure 7(e); Deser and Blackmon, 1995) and the Arctic oscillation (AO) mode, also known as the NAO mode (Figure 7(f); Deser and Blackmon, 1993). These modes are obtained as the first EOF mode in the residual North Pacific and North Atlantic in the JFM season. In order to eliminate the influence of tropical SST variations (i.e. ENSO), the 'residual SST field' linearly independent of ENSO events is used, which can be obtained by subtracting the regressed SST field of the Niño-3.4 index from the raw SST fields; see Yasunaka and Hanawa (2003). The explained variances in the global ocean are 11.4% for the NP mode and 10.3% for the AO mode. The third mode in the NH is a combination of these two modes. Barlow *et al*. (2001) suggested that the NP mode dominated both in the JFM and JAS seasons. Actually, the second mode in the NP in the JAS season has a similar pattern to that in the JFM season. However, even if the spatial patterns of the two seasons are similar to each other, they do not always relate. Since correlation coefficients between the time coefficient of the JFM season and that of the JAS season are not significant with one season leading or lagging (-0.07 for the JFM season leading, and -0.14 for the JAS season leading), we cannot regard them as the same modes.

In summary, four dominant modes are detected in the global SST field: the ENSO mode, the SH trend mode, the NP mode, and the AO mode. We regarded these four modes as the dominant modes with systematic and inherent spatial patterns in the global SST fields.

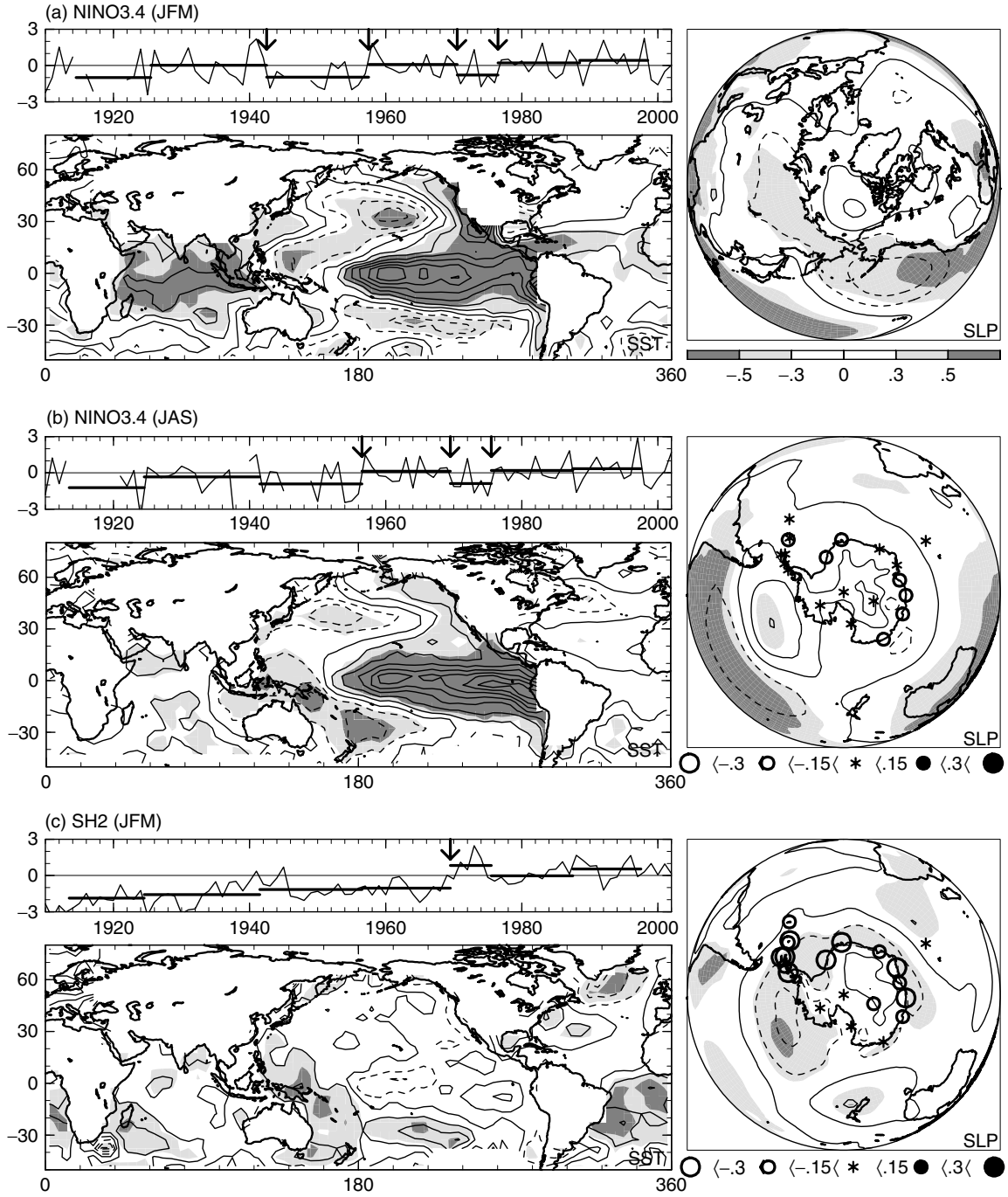

Figure 7. Time series of dominant variations (upper panel) and regression maps of SST (lower panel) and SLP (right panel). (a) The Niño-3.4 index in the JFM season. (b) The Niño-3.4 index in the JAS season. (c) EOF2 in the SH SST field for the period 1958–2002 in the JFM season. (d) As (c), but in the JAS season. (e) EOF1 in the residual North Pacific SST field for the period 1951–2002 in the JFM season. (f) EOF1 in the residual North Atlantic SST field for the period of 1951–2002 in the JFM season. Horizontal bars denote regime means of time series. Arrows show the years showing significant changes at the 90% significance level by the Student *t*-test. Regression maps are obtained by the analyses for the period of 1951–2002, except for SH SLP regressions (1958–2002). Contour interval is 0.1 °C and 1 hPa. Negative contours are dashed. Shadings are given based on correlation coefficients (see the shading bar at the bottom). Circles and asterisks in SLP regression maps denote correlation coefficients of the station SLPs

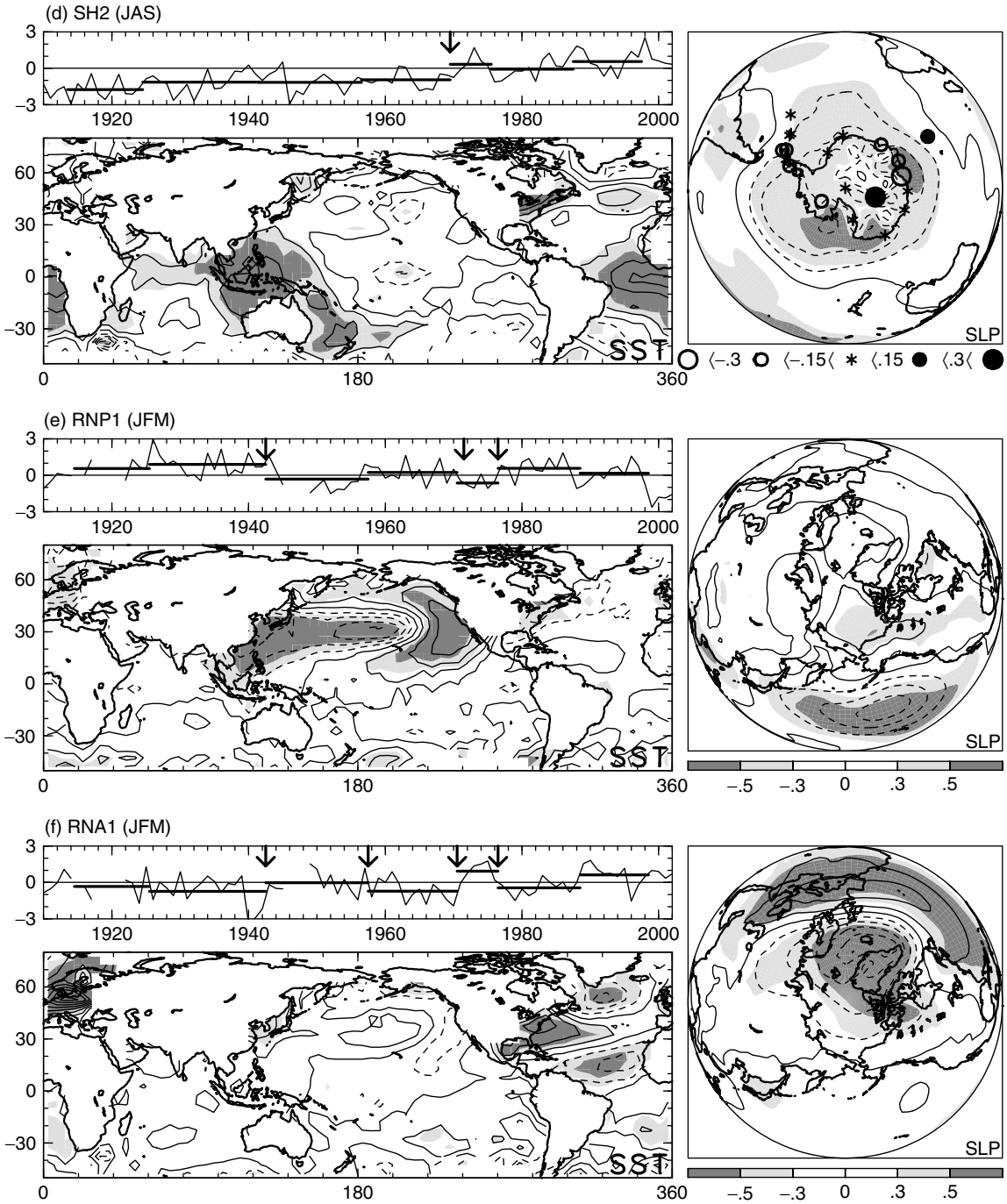

Figure 7. (*Continued*)

4.2. Relation between regime shifts and dominant SST variabilities

We examine whether or not the significant changes at the regime shifts occur in the time coefficients of the dominant SST modes noted in Section 4.1. We calculate mean values of time coefficients of the dominant SST modes obtained in Section 4.1 between the subsequent regime shifts, and check the significance of their

changes at the regime shifts by the Student t-test. The horizontal bars in the time series of Figure 7 show the regime mean and the arrows denote the significant shifts at the 90% significance level. At the regime shifts, the ENSO mode, the NP mode, and the AO mode change their mean states significantly. On the other hand, the SH trend mode does not show significant changes (except for the shift in 1970). Since the changes in the NP mode and the AO mode at the regime shifts occur at the same time as changes of the ENSO mode, the regime shifts would have stronger amplitudes in the North Pacific and the North Atlantic than that of the ENSO events as mentioned in the previous section. The significant change of these three modes was consistent with that detected in the NH by Yasunaka and Hanawa (2003). On the other hand, since there is no dominant mode except for the ENSO mode that relates to the regime shifts in the JAS season, the signals of the regime shifts are not so prominent as those of the JFM season. Since only the ENSO mode relates to the regime shifts in the SH, the signals of the regime shifts are more prominent in the NH than in the SH.

5. CONCLUSIONS

Significant changes appearing widely in the global SST anomaly field were found five times from the 1910s to the 1990s, which is consistent with the NH regime shifts already reported by previous studies (Overland *et al*., 1999; Yasunaka and Hanawa, 2002). It was also found that all the regime shifts happened concurrently with the ENSO events. Although the seasonal evolutions of the regime shifts resemble those corresponding to a series of the evolution of ENSO events, the NH mid-latitude responses are stronger. After the shifts happened, the spatial patterns of SST anomalies after the regime shift persisted until the next shift. From reanalysis of the dominant variation modes in the global SSTs, four modes, which correspond well with the well-known patterns in the ocean–atmosphere system, were identified: the ENSO mode, the SH trend mode, the NP mode, and the AO mode. At the years when regime shifts occurred, not only the ENSO mode, but also the NP mode and the AO mode have shown significant and concurrent changes of mean states on a global scale.

Until now, the decadal-scale variations and the ENSO events have been described individually, which implies independence from each other. However, from the results of the present study, we may suggest that an interaction between the regime shifts and the ENSO events takes place, i.e. the regime shifts are phase-locked in the ENSO events, like the ENSO events are phase-locked in the seasonal cycle of the climate system. This would induce the characteristic features of the regime shift: fluctuation of time intervals between the shifts, an abrupt change like a step function, and an ENSO-like spatial change pattern, as mentioned in the following.

The regime shifts occurred concurrently with the ENSO events. However, all ENSO events did not always associate with the regime shifts, and the ENSO events associated with the regime shifts were not always accompanied by stronger ENSO events. According to Masuda (2002), the ENSO events, which happen only when the background condition is ready to reverse the phase, induce the regime shifts. This implies that the ENSO event acts as a trigger of the regime shift. Furthermore, the time intervals of the regime shifts might not be exactly constant, but could fluctuate to some degree.

Since the tropical Pacific SSTs change from a La Niña (El Niño) condition to an El Niño (La Niña) condition within 1 year at the regime shift, the phase reversal of the decadal-scale variation appears like a step function rather than a sinusoidal function. Furthermore, at the regime shifts, not only the ENSO mode, but also the NP mode and the AO mode change their mean states. This fact is consistent with other previous studies showing that the spatial pattern of the decadal-scale variation resembles, but is not exactly the same as, that of the ENSO (e.g. Zhang *et al*., 1997).

Contrarily, regime shifts would influence the ENSO events. According to the western Pacific oscillator theory (Weisberg and Wang, 1997), the Kelvin wave forced by wind anomalies over the western tropical Pacific propagates eastward along the equator, and forces the SST anomalies to reverse in the central and eastern tropical Pacific. The regressed SSWs in the NP mode show a cyclonic circulation over the western tropical Pacific (see Figure 8). The cyclonic circulation would suppress the growth of the anticyclonic circulation; the

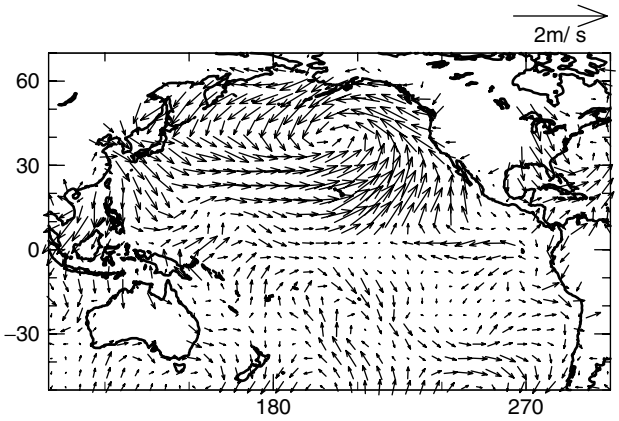

Figure 8. SSW regression maps onto the NP mode

resultant El Niño event would not reverse, but would last for a while. (When the NP mode changes into the negative sign, the anticyclonic circulation would suppress the growth of the cyclonic circulation.) That is, simultaneous phase reversal of the NP mode would cause the ENSO event to last.

However, the present study cannot answer what kind of mechanism sets the background condition inducing the phase reversal of the decadal-scale variation; possibilities include westward propagation of subsurface temperature anomalies in the subarctic region (Masuda, 2002), the subtropical region (Latif and Barnett, 1996), or the tropics (Hasegawa and Hanawa, 2003).

ACKNOWLEDGEMENTS

We thank the members of the Physical Oceanography Laboratory at Tohoku University for their fruitful comments and heartfelt encouragement. We also thank two anonymous reviewers for their helpful comments. SY was supported financially by the Japan Society for Promotion of Science (JSPS) during the course of this study.

REFERENCES

Alexander MA, Deser C. 1995. A mechanism for the recurrence of wintertime midlatitude SST anomalies. *Journal of Physical Oceanography* **25**: 122–137.

Barnston AG, Livezey RE. 1987. Classification, seasonality and persistence of low-frequency atmospheric circulation pattern. *Monthly Weather Review* **115**: 1083–1126.

Barlow M, Nigam S, Berbery EH. 2001. ENSO, Pacific decadal variability, and U.S. summertime precipitation, drought and stream flow. *Journal of Climate* **14**: 2105–2128.

Deser C, Blackmon ML. 1993. Surface climate variations over the North Atlantic Ocean during winter: 1900–1989. *Journal of Climate* **6**: 1743–1753.

Deser C, Blackmon ML. 1995. On the relationship between tropical and North Pacific sea surface temperature variations. *Journal of Climate* **8**: 1677–1680.

Garreaud RD, Battisti DS. 1999. Interannual (ENSO) and interdecadal (ENSO-like) variability in the Southern Hemisphere tropospheric circulation. *Journal of Climate* **12**: 2113–2123.

Hanawa K, Sugimoto S. 2004. 'Reemergence' areas of winter sea surface temperature anomalies in the world's oceans. *Geophysical Research Letters* **31**: L10303. DOI: 10.1029/2004GL019904.

Hasegawa T, Hanawa K. 2003. Decadal-scale variability of upper ocean heat content in the tropical Pacific. *Geophysical Research Letters* **30**: 1272. DOI: 10.1029/2002GL016843.

Horii T, Hanawa K. 2004. A relationship between timing of El Nino onset and subsequent evolution. *Geophysical Research Letters* **31**: L06304. DOI: 10.1029/2003GL019239.

Hurrell JW. 1995. Decadal trends in the North Atlantic oscillation: regional temperatures and precipitation. *Science* **269**: 676–679.

Jones PD, Limbert DWS. 1987. A data bank of Antarctic surface temperature and pressure data. DOE/ER/60397-H2 TR038, Office of Energy Research, Carbon Dioxide Research Division, US Department of Energy, Washington, DC.

Kalnay EM, Kanamitsu M, Kistler R, Collins W, Deaven D, Gandin L, Iredell M, Saha S, White G, Woollen J, Zhu Y, Chelliah M, Ebisuzaki W, Higgins W, Janowiak J, Mo KC, Ropelewski C, Wang J, Leetmaa A, Reynolds R, Jenne R, Joseph D. 1996. The NCEP/NCAR 40-year reanalysis project. *Bulletin of the American Meteorological Society* **77**: 437–471.

Kaplan A, Kushnir Y, Cane MA. 2000. Reduced space optimal interpolation of historical marine sea level pressure: 1854–1992. *Journal of Climate* **13**: 2987–3002.
Karoly DJ. 1989. Southern Hemisphere circulation features associated with El Niño–southern oscillation events. *Journal of Climate* **2**: 1239–1252.
Karoly DJ, Hope P, Jones PD. 1996. Decadal variations of the Southern Hemisphere circulation. *International Journal of Climatology* **16**: 723–732.
Kawamura R. 1994. A rotated EOF analysis of global sea surface temperature variability with interannual and interdecadal scales. *Journal of Physical Oceanography* **24**: 707–715.
Kushnir Y. 1994. Interdecadal variations in North Atlantic sea surface temperature and associated atmospheric circulation. *Journal of Climate* **7**: 141–157.
Lanzante JR. 1996. Resistant, robust and non-parametric techniques for the analysis of climate data. theory and examples, including applications to historical radiosonde station data. *International Journal of Climatology* **16**: 1197–1226.
Latif M, Barnett TP. 1996. Decadal climate variability over the North Pacific and North America: dynamics and predictability. *Journal of Climate* **9**: 2407–2423.
Luo JJ, Yamagata T. 2001. Long-term El Niño–southern oscillation (ENSO)-like variation with special emphasis on the South Pacific. *Journal of Geophysical Research* **106**: 22 211–22 227.
Manabe T. 1999. The digitized Kobe Collection: historical surface marine meteorological observations in the archival of the Japan Meteorological Agency. *Bulletin of the American Meteorological Society* **80**: 2703–2715.
Mantua NJ, Hare SR, Zhang Y, Wallace JM, Francis RC. 1997. A Pacific interdecadal climate oscillation with impacts on salmon production. *Bulletin of the American Meteorological Society* **78**: 1069–1079.
Masuda S. 2002. Role of the ocean in the decadal climate change in the North Pacific. *Journal of Geophysical Research* **107**: 3224. DOI: 10.1029/2002JC001420.
Minobe S. 1997. A 50–70 year climatic oscillation over the North Pacific and North America. *Geophysical Research Letters* **24**: 683–686.
Mo KC. 2000. Relationships between low-frequency variability in the Southern Hemisphere and sea surface temperature anomalies. *Journal of Climate* **13**: 3599–3610.
Namias J, Born RM. 1970. Temporal coherence in North Pacific sea-surface temperature patterns. *Journal of Geophysical Research* **75**: 5952–5955.
Neelin JD, Jin FF, Syu HH. 2000. Variations in ENSO phase locking. *Journal of Climate* **13**: 2570–2590.
Nitta T, Yamada S. 1989. Recent warming of tropical sea surface temperature and its relationship to the Northern Hemisphere circulation. *Journal of the Meteorological Society of Japan* **67**: 375–383.
Overland JE, Adams JM, Boud NA. 1999. Decadal variability of the Aleutian low and its relation to high-latitude circulation. *Journal of Climate* **12**: 1542–1548.
Overland JE, Adams JM, Mofjeld HO. 2000. Chaos in the North Pacific: spatial modes and temporal irregularity. *Progress in Oceanography* **47**: 337–354.
Rasmusson EM, Carpenter TH. 1982. Variations in tropical sea surface temperature and surface wind fields associated with the southern oscillation/El Niño. *Monthly Weather Review* **110**: 354–384.
Rayner NA, Horton EB, Parke DE, Folland CK, Hackett RB. 1996. Version 2.2 of the global sea-ice and sea surface temperature data set, 1903–1994. CRTN 74. Available from Hadley Centre, Met Office, Bracknell, UK.
Rogers JC, van Loon H. 1982. Spatial variability of sea level pressure and 500 mb height anomalies over the Southern Hemisphere. *Monthly Weather Review* **110**: 1375–1392.
Smith TM, Reynolds RW. 2002. Extended reconstruction of global sea surface temperatures based on COADS data (1854–1997). *Journal of Climate* **16**: 1495–1510.
Tachibana Y, Honda M, Takeuchi K. 1996. The abrupt decrease of the sea ice over the southern part of the Sea of Okhotsk in 1989 and its relation to the recent weakening of the Aleutian low. *Journal of the Meteorological Society of Japan* **74**: 579–584.
Tanimoto Y, Xie SP. 1999. Ocean–atmospheric variability over the pan-Atlantic basin. *Journal of the Meteorological Society of Japan* **77**: 31–46.
Tanimoto Y, Iwasaka N, Hanawa K. 1997. Relationship between sea surface temperature, the atmospheric circulation and air–sea fluxes on multiple time scales. *Journal of the Meteorological Society of Japan* **75**: 831–849.
Thompson DJW, Wallace JM. 2000. Annular modes in the extratropical circulation. Part I: month-to-month variability. *Journal of Climate* **13**: 1000–1017.
Thompson DJW, Wallace JM, Hegerl GC. 2000. Annular modes in the extratropical circulation. Part II: trend. *Journal of Climate* **13**: 1018–1036.
Trenberth KE. 1990. Recent observed climate changes in the Northern Hemisphere. *Bulletin of the American Meteorological Society* **71**: 988–993.
Trenberth KE. 1997. The definition of El Niño. *Bulletin of the American Meteorological Society* **78**: 2771–2777.
Trenberth KE, Caron JM. 2000. The southern oscillation revisited: sea level pressure, surface temperature, and precipitation. *Journal of Climate* **13**: 4358–4365.
Watanabe M, Kimoto M. 2000. On the persistence of decadal SST anomalies in the North Atlantic. *Journal of Climate* **13**: 3017–3027.
Weare BC, Navato AR, Newell RE. 1976. Empirical orthogonal analysis of Pacific sea surface temperatures. *Journal of Physical Oceanography* **6**: 671–678.
Weisberg RH, Wang C. 1997. Slow variability in the equatorial west-central Pacific in relation to ENSO. *Journal of Climate* **10**: 1998–2017.
Woodruff SD, Slutz RJ, Jenne RL, Steurer PM. 1987. A comprehensive ocean–atmosphere data set. *Bulletin of the American Meteorological Society* **68**: 1239–1250.
Yasunaka S, Hanawa K. 2002. Regime shifts found in the Northern Hemisphere SST field. *Journal of the Meteorological Society of Japan* **80**: 119–135.

Yasunaka S, Hanawa K. 2003. Regime shifts in the Northern Hemisphere SST field: revisited in relation to tropical variations. *Journal of the Meteorological Society of Japan* **81**: 415–424.
Zhang Y, Wallace JM, Battisti DS. 1997. ENSO-like interdecadal variability: 1900–93. *Journal of Climate* **10**: 1004–1020.

